WSRC-MS-98-00668

# Heat Transfer Modeling of Dry Spent Nuclear Fuel Storage Facilities

by

S. Y. Lee

Westinghouse Savannah River Company
Savannah River Site
Aiken, South Carolina 29808

A document prepared for 1999 NATIONAL HEAT TRANSFER CONFERENCE at Albuquerque, NM, USA from 8/15/99 - 8/17/99.

DOE Contract No. **DE-AC09-96SR18500**

## DISCLAIMER

*WSRC-MS-98-00668*
*This paper is proposed for publication in the proceedings of 1999 ASME National Heat Transfer Conference, Albuquerque, New Mexico, August 15-17, 1999.*

# Heat Transfer Modeling of Dry Spent Nuclear Fuel Storage Facilities

Si Y. Lee
Westinghouse Savannah River Technology Center
773-42A, Rm 184, Savannah River Site
Aiken, SC 29808
Tel (803)725-8462
Fax (803)725-8829
e-mail address: si.lee@srs.gov

## Abstract
The present work was undertaken to provide heat transfer model that accurately predicts the thermal performance of dry spent nuclear fuel storage facilities. One of the storage configurations being considered for DOE Aluminum-clad Spent Nuclear Fuel (Al-SNF), such as the Material and Testing Reactor (MTR) fuel, is in a dry storage facility. To support design studies of storage options a computational and experimental program has been conducted at the Savannah River Site (SRS). The main objective is to develop heat transfer models including natural convection effects internal to an interim dry storage canister and to geological codisposal Waste Package (WP). Calculated temperatures will be used to demonstrate engineering viability of a dry storage option in enclosed interim storage and geological repository WP and to assess the chemical and physical behaviors of the Al-SNF in the dry storage facilities. The current paper describes the modeling approaches and presents the computational results along with the experimental data.

Computation Fluid Dynamics (CFD) approach was used to conduct the thermal performance analyses of the enclosed dry interim storage canister and repository codisposal WP. Two models were developed which are referred to as the interim storage model and the codisposal WP model. The interim storage model is three-dimensional conduction-convection conjugate model to investigate natural convective cooling mechanism of an enclosed interim dry storage canister. The analysis was made for the interim storage canister with various decay heat sources (equivalent to 25 to 35 kW/m$^3$) using various different boundary conditions around the canister wall and different back-filled gases (nitrogen or helium) by using three-dimensional conduction-convection coupled model. The results were also compared with the test data obtained from a full-scale heat transfer experiment conducted at SRS. The codisposal model considers heat transfer mechanisms driven by convection and radiation as well as conduction for a two-dimensional thermal performance analysis of an enclosed repository codisposal WP containing one Al-SNF canister and five High-level Waste Glass Logs (HWGL's). In addition, decay heat sources were developed as a function of storage time for the analysis. For the present analysis, the Boussinesq approximation was used to include the effect of buoyancy-driven natural convection for both of the models. Comparison of the model predictions with the test data can be used to predict reasonably accurate flow and thermal behavior of a typical DOE Al-SNF stored in enclosed dry storage facilities.

## Introduction
The Savannah River Site (SRS) Technology Center has conducted full-scale experimental and computational heat transfer studies for an interim dry storage canister of DOE Aluminum-clad Spent Nuclear Fuel (Al-SNF). In the experiment, the instrumented fuel canister with imbedded electrical heater is surrounded by five unheated dummy canisters, and it is located inside a wind

tunnel. The integral test arrangements are shown in Fig. 1. Radial and axial heat flux/temperature profiles inside the fuel canister, air velocity outside the canister, and ambient temperature were measured. The canister diameter and height are 0.4064m and 0.9144m, respectively. The canister will be filled with helium or nitrogen gas depending on the experiment. The sealed fuel can is located inside the canister and is designed to store four fuel assemblies. Each fuel assembly is separated by the stainless steel grid, and the natural convective flow induced by the buoyancy effect within each compartment of the four fuel assemblies can be communicated with each other only through the top and bottom slot holes inside the canister.

SRS has made a thermal performance analysis to calculate peak temperatures and temperature profiles of codisposal Waste Package (WP) configuration in a geological repository. The analysis results will used to demonstrate compliance with waste acceptance criteria for the SNF storage systems and as input to assess the chemical and physical behavior of the Al-SNF forms within the WP. The leading codisposal WP design proposes that a central DOE spent nuclear fuel (SNF) canister be surrounded by five Defense Waste Process Facility (DWPF) glass log canisters, that is, High-level Waste Glass Logs (HWGL's), and placed into a WP in the Mined Geologic Disposal System (MGDS). The waste package is cylindrical with a diameter of about 6 ft. A DOE SNF canister having about 17 inch diameter and about 10 ft length is placed along the central horizontal axis of the WP. The five HWGL's, each with a 2 ft diameter and 10 ft length, will be located around the peripheral region of the DOE SNF canister within the WP container. The codisposal WP will be laid down horizontally in a drift tunnel repository as shown in Fig. 2.

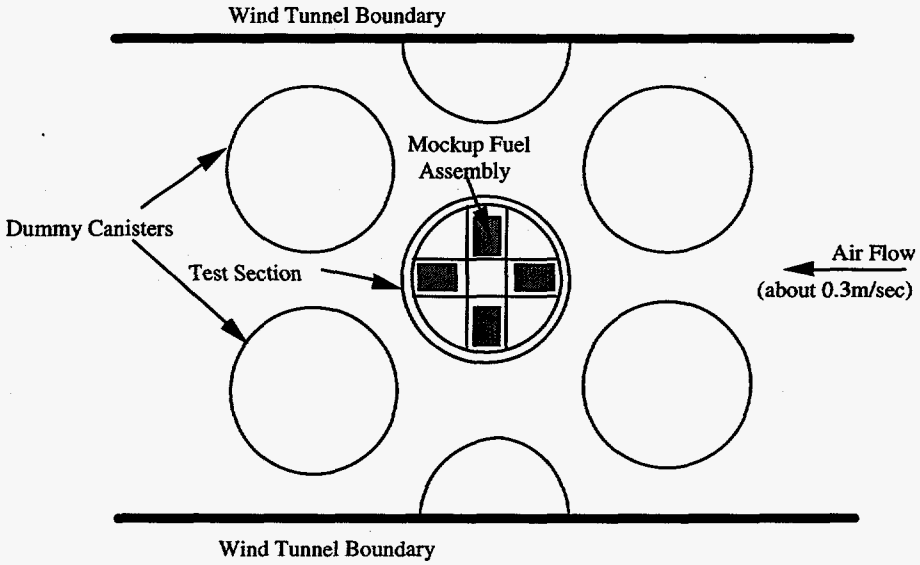


Figure 1. Test section geometry in the prototypic experiment for the interim dry storage facility.

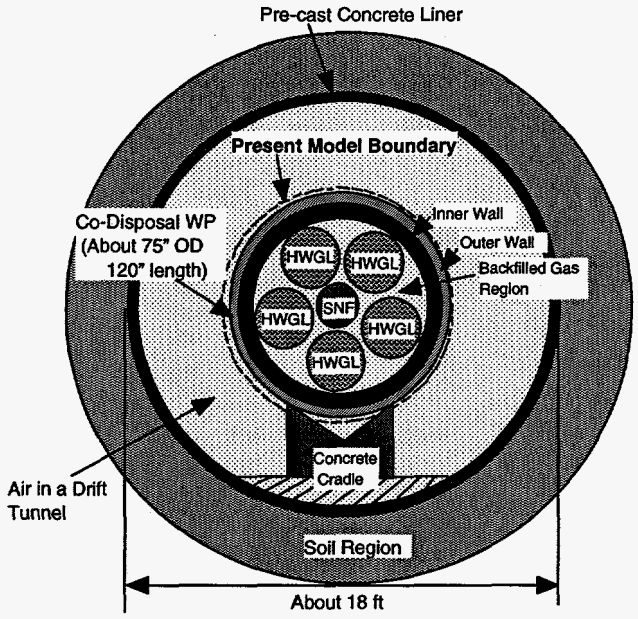


Figure 2. Horizontal emplacement of codisposal waste package in a geological tunnel repository.

The transient decay heat loads were recently developed for this analysis. The heat loads included the Al-SNF assemblies in the direct form and the HWGL. The Al-SNF heat loads were computed by the ORIGEN code under SCALE 4.2 system. Reference design conditions were assumed to perform the analyses.

The objective of this study is to develop the heat transfer model for the dry Al-SNF storage canister using a Computational Fluid Dynamics (CFD) approach and to benchmark it against the SRS test data for various boundary conditions. The objective is also to develop the thermal model used to investigate the physical cooling mechanism about decay heat transport through the WP to the environment in a geological repository. These simulation results will provide verification that the models can predict reasonably accurate thermal and gas flow behavior within a dry storage canister of a typical foreign research reactor fuel assembly, such as the Material and Testing Reactor (MTR). It is expected that the present approach can be used to accurately predict temperatures of similar fuels in various dry storage configurations.

**Descriptions of Modeling Approaches and Solution Methods**

The heat generated by the radioactive decay process of SNF in a dry storage container will be cooled by back-filled gas medium and eventually will be transported to the surrounding environment or geological repository medium through the physical mechanisms of conduction, convection, and radiation heat transport processes. In this situation the temperature gradient at the wall is dependent on the gas flow field driven by the density gradient at the boundary layer since the temperature gradient is dependent on the rate at which the gas fluid convects the heat away. Thus energy transport is coupled to the momentum transport through the wall interface of the solid and fluid regions. The complicated geometrical configurations of the Al-SNF storage facilities with decay heat sources require a multi-dimensional heat transfer model with a high computational efficiency. CFX code has been used as a tool to model the prototypic configurations of the storage facilities.

A steady-state solution is desired for the present work, and this can be achieved either by advancing the governing equation set through a sequence of time steps or by dropping the transient term completely from the equations and using a purely iterative approach. For the present analysis, the first approach, that is, the quasi-steady approach was used by solving the transient equations. This approach was proven to be an efficient method in the V&V test of the code (Lee, 1996). The analysis was mainly made for the temperature distributions and the buoyancy-driven flow field induced by the temperature gradient within an enclosed package. Temperature decreases rapidly due to the convective cooling effect within a boundary layer region. The flow is a buoyancy-induced motion resulting from body forces acting on density gradients which, in turn, arise from temperature gradients in the fluid. The gravitational body force is oriented in the negative z-direction for the present analysis. The transient equations governing the present problems under the Cartesian coordinate system are shown below.

For the mass continuity,

$$\frac{\partial \rho}{\partial t} + \sum_{i=1}^{3}\left\{\frac{\partial(\rho u_i)}{\partial x_i}\right\} = 0 \qquad (1)$$

where the variables with the subscript, i = 1, 2, or 3, correspond to those of the x-, y-, or z-direction, respectively.

For the momentum equation in tensor notation,

$$\rho\left(\frac{\partial u_i}{\partial t} + u_j\frac{\partial u_i}{\partial x_j}\right) = \frac{\partial \sigma_{ij}}{\partial x_j} + X_i \qquad (2)$$

where the variables with the subscript, i (or j, k) = 1, 2, or 3, correspond to those of the x-, y-, or z-direction, respectively. $\sigma_{ij}$ is the stress tensor and $X_i$ the body force term.

$$\sigma_{ij} = -\left(P + \frac{2}{3}\mu\frac{\partial u_k}{\partial x_k}\right)\delta_{ij} + \mu\left(\frac{\partial u_i}{\partial x_j} + \frac{\partial u_j}{\partial x_i}\right)$$

$$\delta_{ij} = \begin{cases} 1 & \text{for } i = j \\ 0 & \text{for } i \neq j \end{cases}$$

$X_1 = X_2 = 0$ for the present model.

For the energy equation,

$$\rho\frac{Dh}{Dt} - \sum_{i=1}^{3}\left\{\frac{\partial}{\partial x_i}\left(k\frac{\partial T}{\partial x_i} - q_{r,i}\right)\right\} - \frac{DP}{Dt} - \Phi - q''' = 0 \qquad (3)$$

where $\Phi$ is viscous dissipation term, h thermodynamic enthalpy, and q''' heat generation source term. $q_{r,i}$ in eq. (3) is net radiative heat flux in the i-direction. The viscous dissipation term is not included in the present model.

For the present analysis, the Boussinesq approximation was used for the gravitational term in the momentum equation to include the buoyancy-induced natural convection. It is a two-part approximation: It neglects all variable property effects in the governing equations and it approximates the density difference term with a simplified equation of state, that is, the gravity term in the z-direction, $X_3 = -\rho g$, in eq. (2) is replaced by the following relation:

$$\rho g = \rho_\infty\{1 - \beta(T - T_\infty)\}g \qquad (4)$$

where $\beta$ is thermal expansion coefficient, and $\rho_\infty$ is the density at $T = T_\infty$.

The detailed descriptions of the solution approaches for the two different configurations are provided below.

**I. Interim Storage Model**

Detailed geometrical configurations are shown in Fig. 3. Natural convective flow regime for the He-cooled or $N_2$-cooled design shown in Table 1 may be estimated based on the non-dimensional quantity, Grashof number ($Gr_Z$), which is the parameter describing the ratio of buoyancy to viscous forces. The Grashof number performs much the same function for natural convection flow as the Reynolds (Re) number does for forced convection. Under normal conditions one may expect that the laminar-to-turbulent transition will take place at about $Gr_L \approx 10^9$.

For He-cooled canister (Case-1 to Case-4),

$$Gr_L = \frac{g\beta L^3 (T_w - T_\infty)}{\nu^2} \qquad (5)$$

$$\approx 1.40 \times 10^7 < 1.0 \times 10^9 \text{ (laminar flow)}$$

where L = characteristic length parameter,

$\beta$ = thermal expansion coefficient (= $2.85 \times 10^{-3}$ $K^{-1}$),

$T_\infty$ = ambient temperature,

$\nu$ = kinematic viscosity (= $1.593 \times 10^{-4}$ $m^2$/sec).

For $N_2$-cooled canister (Case-5 to Case-7),

$Gr_L \approx 3.60 \times 10^8$

where $\beta = 2.50 \times 10^{-3}$ $K^{-1}$,

$\nu = 2.594 \times 10^{-5}$ $m^2$/sec.

This corresponds to the near-transition flow according to the literature information (Kays and Crawford, 1980). For the present analysis, natural convection regime within the canister is assumed to be laminar.

For computational efficiency, only 90° sector of the test geometry was modeled in a three-dimensional computational domain by using symmetrical condition of internal geometry for a single canister. Two symmetrical planes were taken through the center of the x- and y- planes (see Fig. 3). The dimensions of the canister, as modeled, are presented in Figs. 3. The validity of a 90° sector model was initially of some concern due to asymmetry of published data on the variation of the heat transfer coefficient around a tube in crossflow due to the flow separation effect near the 90° and 270° locations. Thus, the heat flux crossing the symmetry boundaries of the quadrant model would not be zero as assumed.

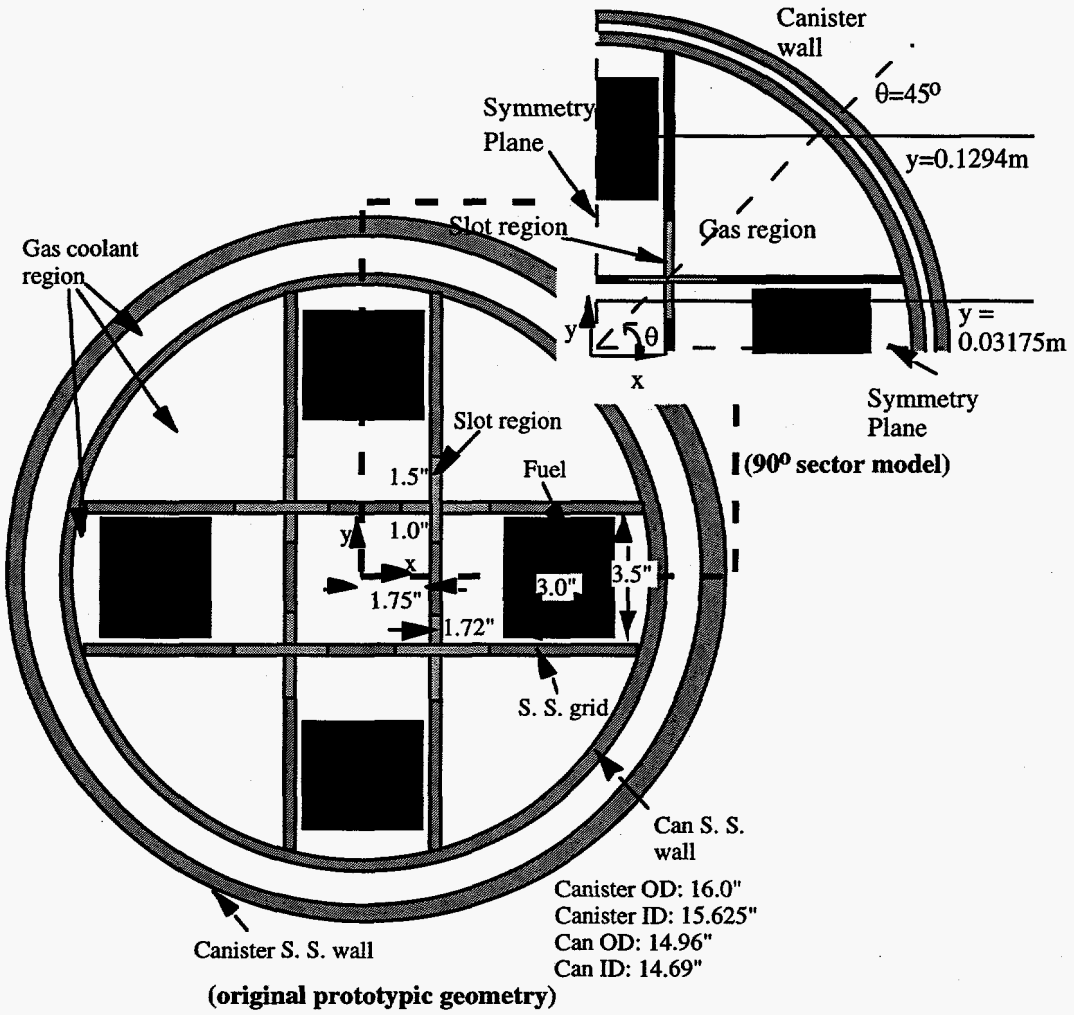


Figure 3. Cross-sectional view of 90° sector model (slot is open only near top and bottom regions).

Table 1. Model conditions for the present analysis of the interim storage canister.

| Cases | Gas within canister | Boundary conditions at canister outer wall surface* | Ambient temperature | Internal heat source (W/bundle) |
|---|---|---|---|---|
| **Case-1 (Test No. I-6)** | He | Variable (6.7 to 8.9 $W/m^2K$) | 21.5 °C | 137.5 |
| **Case-2 (Test No. I-4R)** | He | Variable (6.4 to 8.5 $W/m^2K$) | 21.1 °C | 97.0 |
| **Case-3 (Test No. I-14)** | He | Variable (16.7 to 19.6 $W/m^2K$) | 22.4 °C | 99.9 |
| **Case-4 (Test No. I-15)** | He | Variable (14.5 to 16.6 $W/m^2K$) | 21.9 °C | 100.5 |
| **Case-5 (Test No. II-13)** | $N_2$ | Variable (6.1 to 8.6 $W/m^2K$) | 23.5 °C | 92.6 |
| **Case-6 (Test No. I-13R)** | $N_2$ | Variable (6.8 to 8.1 $W/m^2K$) | 23.0 °C | 92.8 |
| **Case-7 (Test No. I-21)** | $N_2$ | Variable (12.5 to 13.4 $W/m^2K$) | 21.2 °C | 84.8 |

*: Boundary conditions at top and bottom surfaces are assumed to be adiabatic.

However, the results of the tests indicate that at least for the tests with the canister rotated 45°, the heat flux distribution was nearly symmetrical and results of tests with the canister with and without rotation had similar fuel mockup temperatures. This means that for the mixed convection case, the natural convection effect on the canister wall heat transfer predominated over the forced convection effect. From the fact that the mockup heater temperatures were very nearly equal, it is suggested that the use of a 90° model is acceptable.

The fuel region was simulated by using 18 plate MTR-type fuel element in the Separate Effects tests. The mockup fuel plates were made of 1.27mm thick aluminum, and spaced 3.2mm apart. This fuel region was modeled as a homogeneous region by using an effective thermal conductivity ($k_{eff}$) obtained from the Separate Effects test. This was also necessary to reduce the number of computational mesh points for the fuel region. For all other regions such as grid regions around wall touch zones and extended fuel region, the effective thermal conductivity was obtained as the volume averaged value of the metal and gas constituents. The narrow gas space (gap distance ≈ 8.4mm) between the inner and outer canister walls is assumed to be conduction-dominant. The interior of the canister in the model is filled with helium or nitrogen gas.

Seven different cases studied here are shown in Table I. They are $N_2$-/He-gas filled spent nuclear fuel canisters with an internal heat source in the fuel region and a variable wall heat transfer coefficient. Test data (Lee, 1996) showed that wall heat transfer coefficient was varied with azimuthal position around the canister surface, which provided the boundary conditions to the compuational model for Case-1 to Case-7. The model actually used the discretized wall boundary conditions for computational efficiency. Top and bottom surfaces of the storage canister are assumed to be adiabatic.

The three-dimensional geometry file was created using the multi-block preprocessor of the CFX code under the body-fitted coordinate system, which allows the treatment of non-orthogonal geometry. An effort was made to build a non-uniform fine meshing with progressive change of grid size near the conduction-convection interface to capture detailed temperature and velocity boundary layer behavior. The program was run under the SGI workstation platform because of the large memory requirements.

For the present analysis, an optimum grid of 89632 cells was established from the grid sensitivity analysis. The canister consists of 8 different layers and 32 mesh grids along the z-direction as illustrated in Fig. 4. Adequacy of grid fineness for the present computational domain is illustrated in Fig. 5. Thermal radiation effect is assumed to be negligible compared to conduction and convection heat transfer mechanism since average temperature in the present analysis is generally low (McAdams, 1954) and benchmarking results based on the conduction-convection coupled model are in good agreement with the test data.

**II. Codisposal WP Model**

Thermal performance analysis for the codisposal WP design including Al-SNF has been performed as a function of storage time for various boundary conditions by using a parametric analysis approach.

For a typical reference design condition such as helium-cooled, intact codisposal WP as shown in Table 2,

$$Gr_L = \frac{g\beta L^3 (T_w - T_\infty)}{\nu^2} \qquad (6)$$

$$\approx 4.0 \times 10^7 < 1.0 \times 10^9 \quad \text{(laminar flow)}$$

where L = characteristic length parameter (=1.7545 m),

$\beta$ = thermal expansion coefficient (= 2.00 x $10^{-3}$ $K^{-1}$),

$T_w$ = wall temperature,

$T_\infty$ = ambient temperature,

$\nu$ = kinematic viscosity (= 2.91 x $10^{-4}$ $m^2$/sec).

This corresponds to the laminar flow according to the literature information (Kays and Crawford, 1980). For the present analysis, natural convection regime internal to the WP is assumed to be laminar.

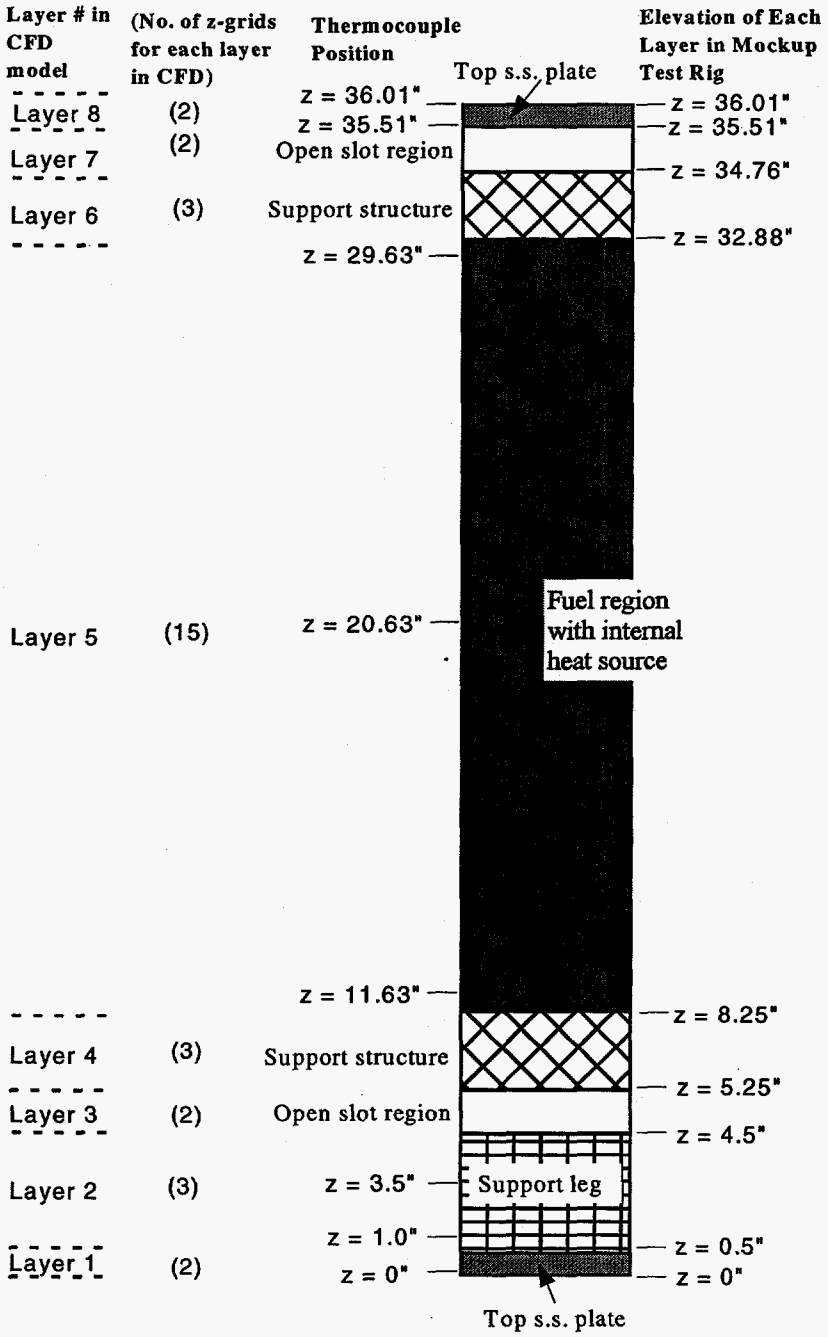


Figure 4. Experimental thermocouple positions and elevation heights of 8 layers in the computational model.

The initial storage time, "Year 0", is defined as the time the canister leaves the site and is put into the WP canister and emplaced in the repository. For the present analysis, initial times for the SNF and the HWGL are assumed to be 10 years cooling time after fuel discharge from the reactor and after the production of high-level waste glass log. The WP temperatures are then computed for selected times during the first 2000 years after emplacement in the repository. A quasi-steady state temperature distribution is assumed for each selected time since the package transient temperatures will reach equilibrium in a few days. The present modeling boundary is shown in Fig. 2. For the reference design conditions shown in Table 2, the physical cooling mechanism has been investigated to understand how decay heat energy is transported through the WP to the geological environment. Specifically, how the waste package temperature affects the buoyancy-driven natural circulation inside the WP, and what is the most dominant mode of thermal energy transport for the present codisposal WP configuration are investigated. This information may be important to assess corrosion degradation of the WP and to determine the movement of moisture outside the WP boundary. The present analysis considers conduction, convection, and radiation cooling mechanisms inside the codisposal WP container by using a two-dimensional approach.

A two-dimensional, conduction-convection model combined with radiation was considered using uniformly-distributed heat generation sources within HWGL and SNF canisters to predict the package thermal performance within a geological repository. A typical natural convective heat transfer coefficient (h) was used as an external wall boundary condition for the present analysis.

$$Nu_L = \frac{hD}{k} = C\left(Gr_L\, Pr\right)^m \qquad \text{for } Gr_L\, Pr > 10^4 \qquad (7)$$

For the present geometrical configuration shown in Fig. 2, C=0.525 and m=0.25 are given by Chapman (1974) using the experimental data. From eq. (7), heat transfer coefficient (h) is about 1.5 $W/m^2{}^\circ C$ corresponding to $Nu_L \approx 97$ conservatively under the present conditions.

The governing equations are provided in eq.(1) through eq.(4). It is assumed to have no solid conduction paths among the SNF and HLWG canisters such that the HLWG canisters, the SNF canister, and the codisposal waste package inner wall do not touch each other since final geometrical configuration for the codisposal WP is neither confirmed nor available yet. A half-cylinder model of the codisposal WP shown in Fig. 2 was used as a computational domain for computational efficiency by imposing symmetrical boundary conditions along the centerline of the WP. An optimum grid of about 10000 cells was established from the grid sensitivity using the same method as discussed earlier.

The segregated solution technique was selected for the efficient computations of the interim storage and geological codisposal WP problems with internal heat sources.

Table 2. Reference design conditions of codisposal WP for the present thermal analysis.

| Design Parameters | Design Conditions |
|---|---|
| • Back-filled gas inside / outside of SNF canister in codisposal WP | • Helium gas inside and outside of SNF canister |
| • Initial reference time (storage time: "Year 0") | • 10 years cooling time since discharge from reactor and production of HWGL |
| • Internal structure of the WP container | • Intact codisposal geometry |
| • Repository ambient temperature | • 100 °C |
| • WP location in a repository tunnel | • Center of a drift tunnel |

Numerical methods for the present analysis were described in detail in the previous work (Lee, 1996). Non-staggered grid approach for each control volume was used since the staggered grid approach prohibitively requires large storage of geometric information to describe a fully non-orthogonal grid.

The overall energy balance should be checked to demonstrate the adequacy of the grid used. This was done by using equation (8).

$$R(W) = -\int_{A_W} q''_w dA + q''' V_F \qquad (8)$$

where $q_w$ is heat flux along the wall surface boundary, and $A_W$ and $V_F$ are total wall surface area and fuel region volume, respectively.

Volumetric heat source term, q''', in equation (8) is given by the code input. For all the seven cases considered here, energy residual (R) is less than about 0.5 watt. For instance, the residual results for the Case 1 of the interim storage canister are shown as function of grid number in Fig. 5.

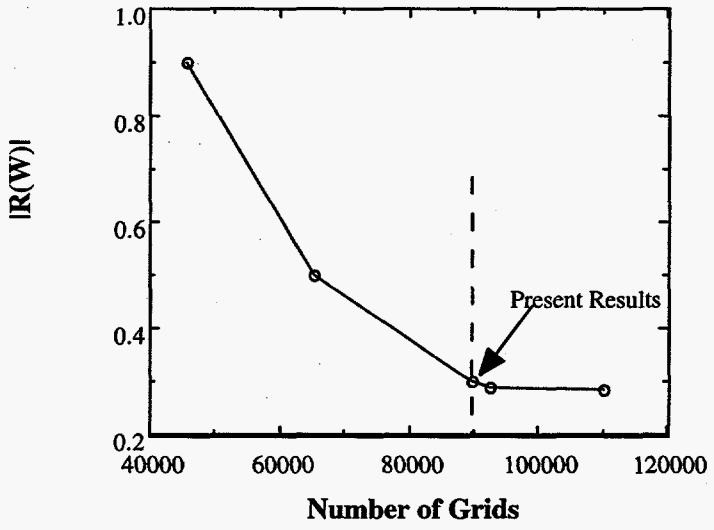


Figure 5. Adequacy of the grid fineness for the present analysis (R(W) is energy residual computed by Eq. (8)).

**Results and Discussions**

The three-dimensional analysis was made for the seven cases of the interim storage test canister, Case-1 to Case-7, with q'''=85 to 138 watts per MTR fuel element (equivalent to about 22 to 35 $kW/m^3$) and $h_{wall}$ = variable (6.1 to 19.6 $W/m^2K$). In addition, the two-dimensional conduction-convection conjugate model combined with radiation was developed to investigate the detailed cooling mechanism of Al-SNF assemblies and HWGL packages completely enclosed inside the container in relation to the thermal performance of the repository codisposal WP. The results for each of the two models are presented and discussed below, respectively.

**I. Interim Storage Canister:**

The computed maximum fuel and canister wall surface temperatures were compared with SRS experimental data for the conduction-convection coupled problem. The results for the seven cases are presented in Table 3. Maximum temperature for $N_2$-cooled canister (Case-5 to Case-7) is higher than that of He-cooled canister (Case-1 to Case-4) since He thermal conductivity is

about 6 times higher than that of $N_2$ gas. The previous results (Lee, 1996) showed that natural convective cooling effect for nitrogen-cooled design was much higher than that of helium-cooled design, which is consistent with the test results.

Table 3. Comparison of maximum temperature and canister outer wall temperature predicted by the CFD model with the test data for each case.

| Cases | CFD Results | | Test Results | |
|---|---|---|---|---|
| | Maximum (°C) | Wall Surface (°C) | Maximum (°C) | Wall Surface (°C) |
| **Case-1** | 167 | 81 | 165 | 88 |
| **Case-2** | 128 | 66 | 136 | 72 |
| **Case-3** | 106 | 41 | 115 | 44 |
| **Case-4** | 114 | 45 | 117 | 47 |
| **Case-5** | 197 | 60 | 196 | 67 |
| **Case-6** | 197 | 60 | 210 | 68 |
| **Case-7** | 171 | 39 | 179 | 44 |

The gas near the central region within an enclosed canister is moving upward like a gas plume, while the gas near the cooler space like the near-wall region is moving downward due to the gravity effect. Figure 6 illustrates overall gas flow pattern over the entire flow domain within the canister from the computational results for Case-1 to Case-7. The results clearly show that there are two main flow circulation loops within the canister. The hot gas near the central region goes up due to buoyancy and passes through the open top slot region (0.75" in slot height) into the near-wall corner of the vacant quadrant, and it then goes downward along the near-wall corner region. The gas cooled by the convective wall boundary condition reaches the bottom slot region, and it is divided into two gas upstreams. One gas stream goes up through the corner near the empty quadrant adjacent to the mockup fuel element, and the other goes up along the central region of the canister through the open bottom slot.

Figure 7 presents temperature predictions for fuel center region along the vertical direction in Case-1 and Case-5. The predictions are also compared with the SRS test data. The results show that maximum fuel temperature occurs near the top of the mockup fuel element. Figure 8 shows comparison of results for the predicted temperature distribution and the test data for the two cases along x=0.1294m line (see Fig. 3 for the line location) on the mid-plane of the fuel region. It is noted that gas temperature of Case-1 (He-cooled design) changes smoothly from the hot side to the cold and the gas velocity profile corresponding to this temperature distribution is shown to be laminar as expected. The results are shown in Fig. 9. The effect of fluid motion on the net heat transfer rate q" entering the system through the heated portion of the driving wall was evaluated and cast in dimensionless form as a Nusselt number (Nu) along the vertical wall.

$$Nu = \frac{q_{wall}''}{k(\Delta T)} = -\int_0^{1.0} \left(\frac{\partial \theta}{\partial \eta}\right)_{wall} d\eta \qquad (9)$$

Dimensionless parameters used in eq. (9) were defined as follows:

$\theta = (T - T_b)/(T_t - T_b)$, $\eta = (z/L)$,

$T_b$ = temperature at the bottom of the mid-plane,

$T_t$ = temperature at the top of the mid-plane, and L = heated vertical length.

The numerical integration of eq. (9) was performed after the quasi-steady temperature field was obtained. The results were compared with the literature correlations as shown in Fig. 10.

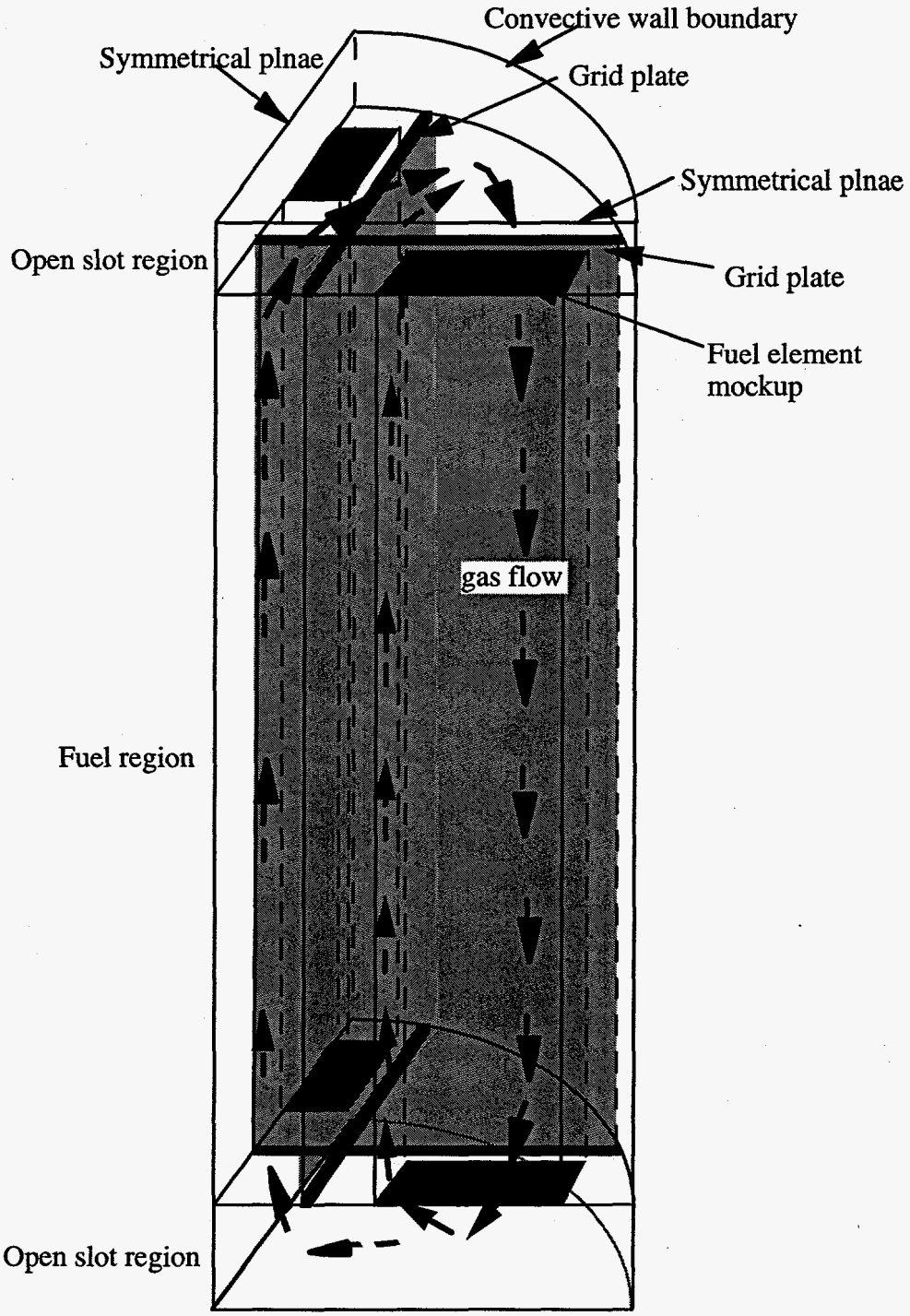


Figure 6. Overall gas flow pattern due to natural convection in the 90° sector model of an enclosed canister.

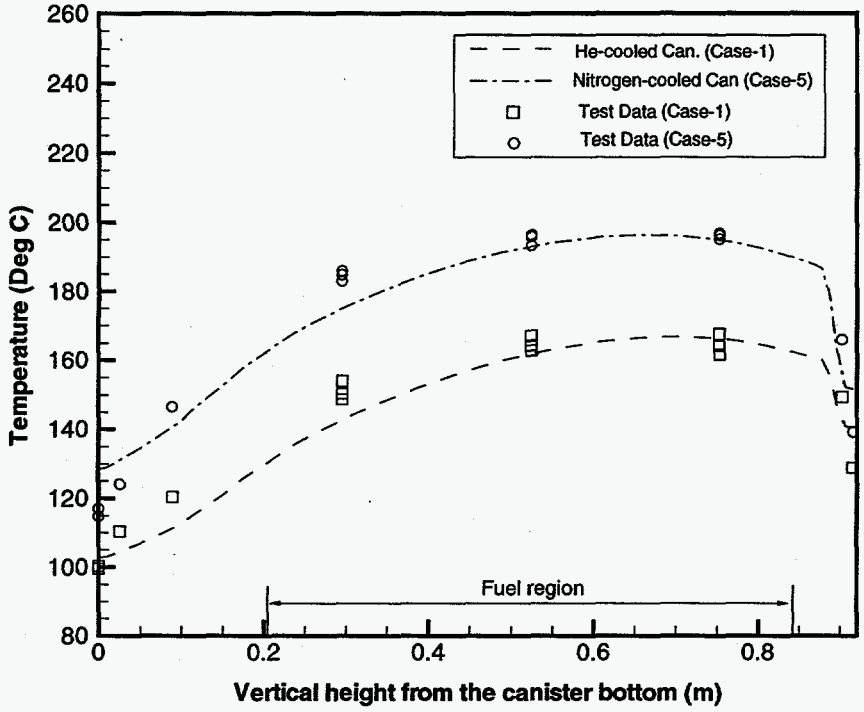


Figure 7. Temperature profiles for fuel center region along the vertical direction.

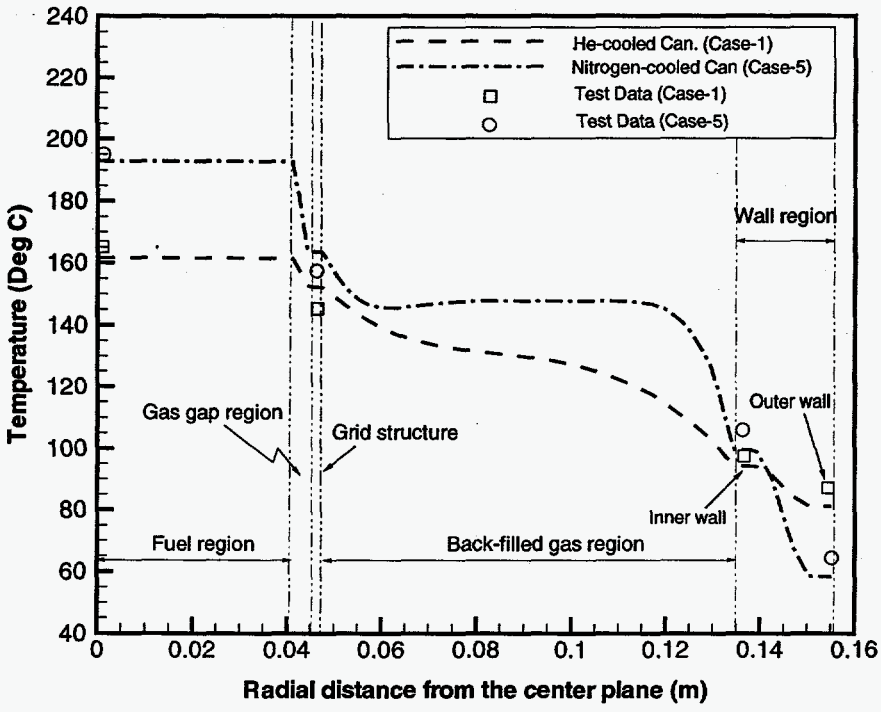


Figure 8. Temperature distributions along the fuel mid-plane (x = 0.1294 m in Fig. 3).

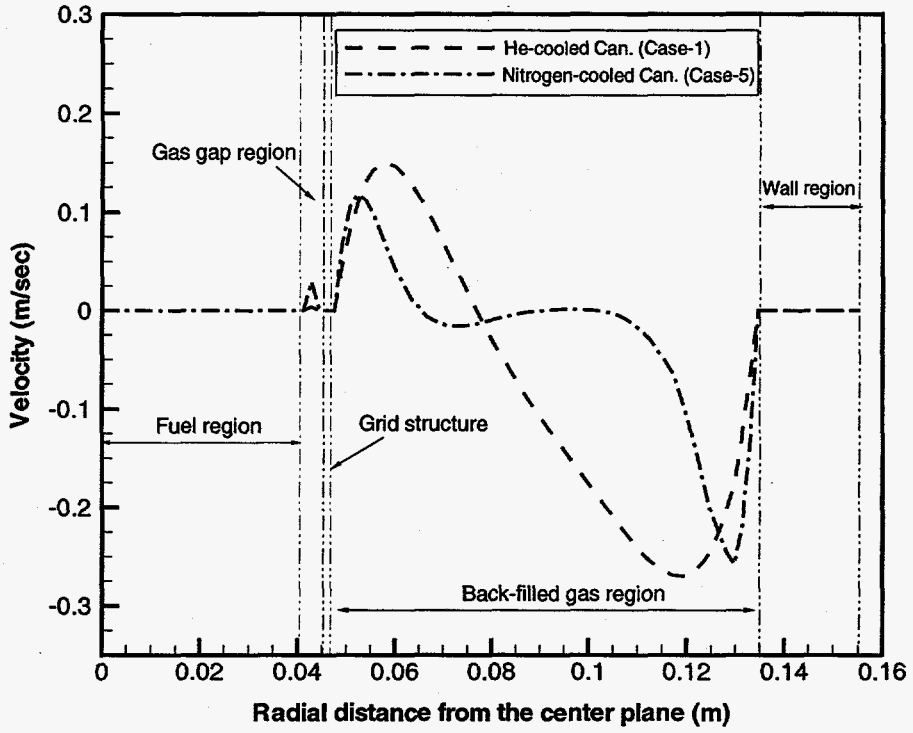


Figure 9. Velocity profile along the fuel mid-plane (x = 0.1294 m in Fig. 3).

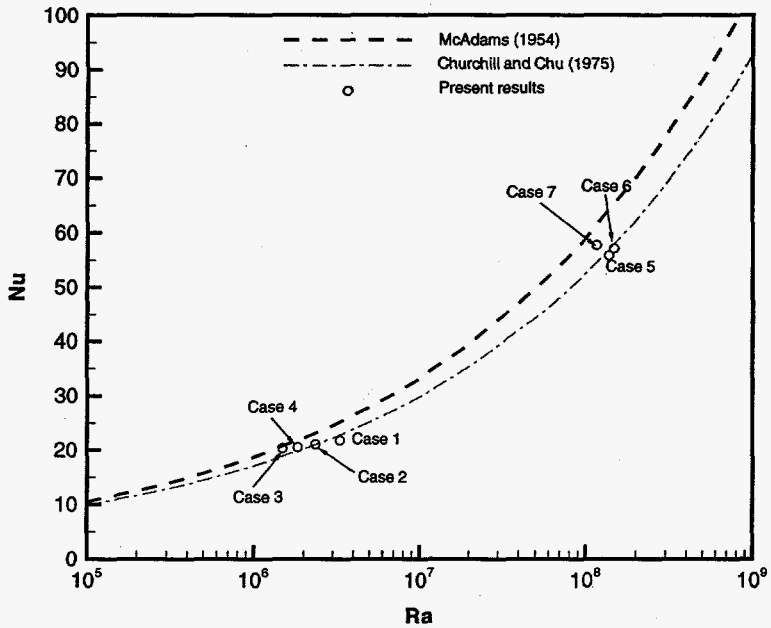


Figure 10. Comparison of the present analysis results with the literature correlations.

From the computational results for Case-5 to Case-7, it was found that there were small vortices near the top/bottom open slot region. Spatial temperature and velocity gradients near the solid-fluid interface for $N_2$-filled canisters are much larger than those of He-filled canisters although internal heat sources in $N_2$-filled canisters are smaller than those of He-cooled canisters (see Fig. 8). These results indicate that the natural covective flow regime for the $N_2$-cooled canister is close to the transition to the turbulent flow ($Gr_z \approx 10^9$) as described in the previous section.

Finally, the model predictions for the prototypic dry spent nuclear fuel storage canister tests are benchmarked against the SRS test data. The benchmarking results for all the cases (Case-1 through Case-7) are shown to be in good agreement with the test.

**II. Codisposal WP:**

The thermal performance analyses were made based on the decay heat sources for the reference conditions shown in Table 2. Al-SNF decay heat loads computed by the ORIGEN code are shown as function of storage time in Table 4. The WP temperatures were then computed for selected times during the first 590 years after emplacement in the repository. The results showed that radiation is the most dominant cooling mode among the three energy transport processes, conduction, convection, and radiation, under the present WP situation. The analysis was performed based the two models, which are referred to as the detailed model and the baseline model. The detailed model considers all the possible three heat transfer modes, while the baseline model neglects convective cooling mechanism in the analysis. The detailed model predicts about 303 °C for the maximum temperature of the codisposal WP at 0 years of storage time under the reference conditions. The radial temperature profiles performed by the two models are compared in Fig. 11. The results of the detailed model provided quantitative estimation of the conservatism imbedded in the baseline model. The detailed model gave highly non-uniform package wall surface temperature such that top surface temperature of the WP is about 10 °C higher than that of the bottom surface. The detailed model results also showed that temperature gradients across the HWGL regions are much smaller compared to the baseline model results for a given elevation height from the bottom of the WP in a horizontal storage position. This is one of the evidences of the buoyancy-driven circulation internal to the codisposal WP. This phenomenon may be important in relation to the movement of water moisture around the WP surface inside a drift tunnel since the moisture directly affects corrosion of the WP materials. Peak temperatures with the detailed model are about 1 °C lower than those of the baseline model under the reference conditions.

Figure 12 shows radial temperature distributions of the codisposal WP under the reference conditions as a function of storage time using the baseline model. Maximum temperature for the baseline model is about 304 °C at the initial storage time (0 years of storage time). The present work was also conducted over a wide range of possible repository temperature conditions. Average temperature of the WP was found to be very close to geological ambient temperature at about 1000 years of storage time after emplacement of the WP in a repository.

Table 4. Decay heat source in SNF canister and HWGL regions for the codisposal WP.

| Storage Time (yrs) | Assembly Power (W/assembly) | Power per HWGL (W) | Total Power for SNF Can. (W) | Volumetric SNF Power (W/m3) | Volumetric HWGL Power (W/m3) |
|---|---|---|---|---|---|
| 0 | 8.58 | 472.3 | 549.12 | 2735.752 | 530.913 |
| 10 | 6.53 | 375.99 | 417.92 | 2082.105 | 422.651 |
| 20 | 5.243 | 301.35 | 335.552 | 1671.742 | 338.748 |
| 50 | 2.83 | 159.5 | 181.12 | 902.352 | 179.294 |
| 90 | 1.382 | 73.1 | 88.448 | 440.654 | 82.1718 |
| 190 | 0.487 | 16.81 | 31.168 | 155.281 | 18.896 |
| 290 | 0.3442 | 7.09 | 22.0288 | 109.749 | 7.9699 |
| 590 | 0.2218 | 1.98 | 14.1952 | 70.721 | 2.2257 |
| 990 | 0.1468 | 1.14 | 9.3952 | 46.808 | 1.2815 |
| 1990 | 0.0794 | 0.72 | 5.0816 | 25.317 | 0.8094 |
| 2990 | 0.063 | 0.62 | 4.032 | 20.088 | 0.6969 |
| 5990 | 0.0505 | 0.52 | 3.232 | 16.102 | 0.5845 |
| 9990 | 0.041 | 0.43 | 2.624 | 13.073 | 0.4834 |
| 19990 | 0.0265 | 0.3 | 1.696 | 8.4496 | 0.3372 |
| 49990 | 0.0103 | 0.16 | 0.6592 | 3.2842 | 0.1799 |
| 99990 | 0.0034 | 0.11 | 0.2176 | 1.0841 | 0.1237 |

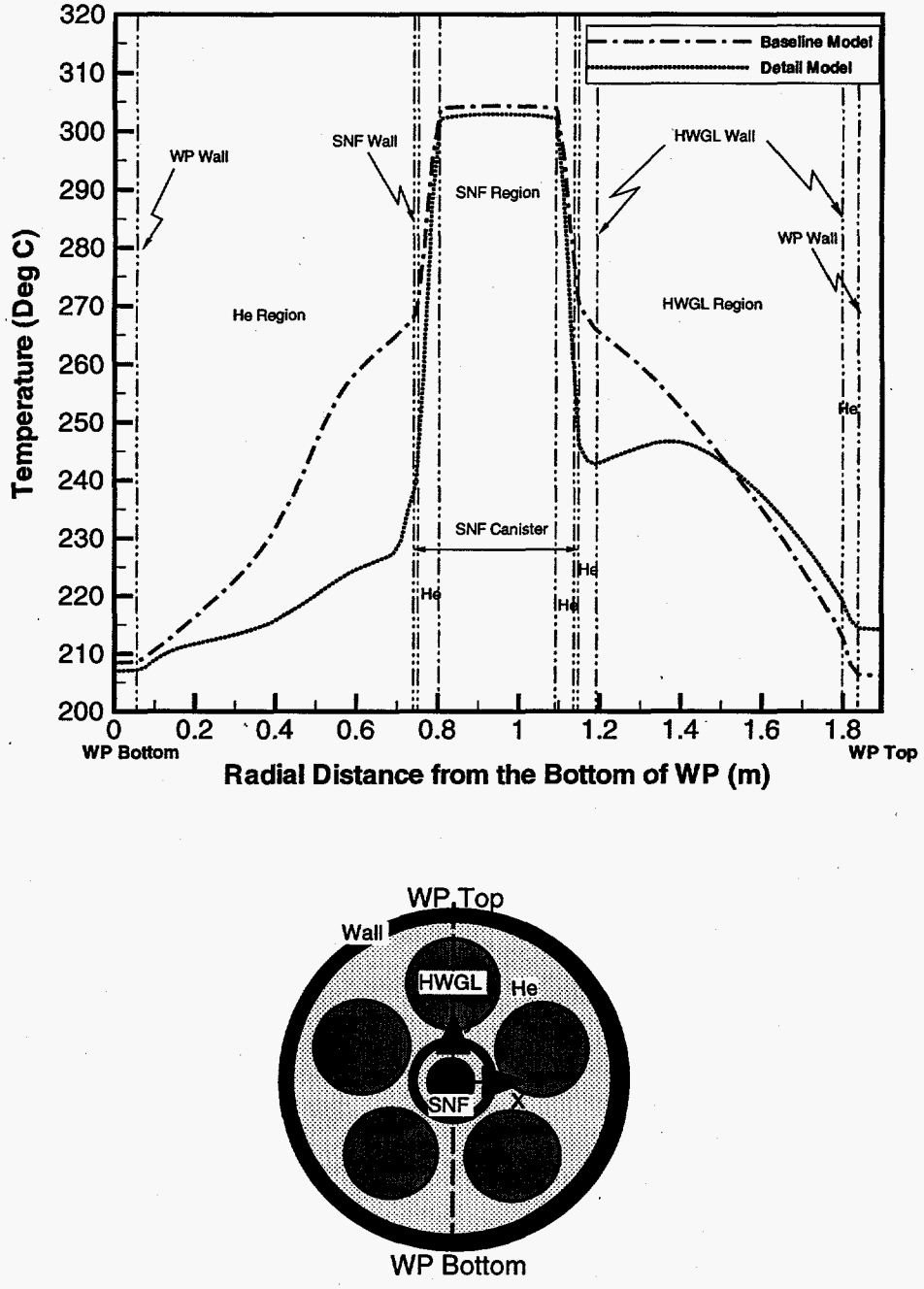


Figure 11. Comparison of centerline temperature distributions based on the baseline model and the detailed model for the codisposal WP.

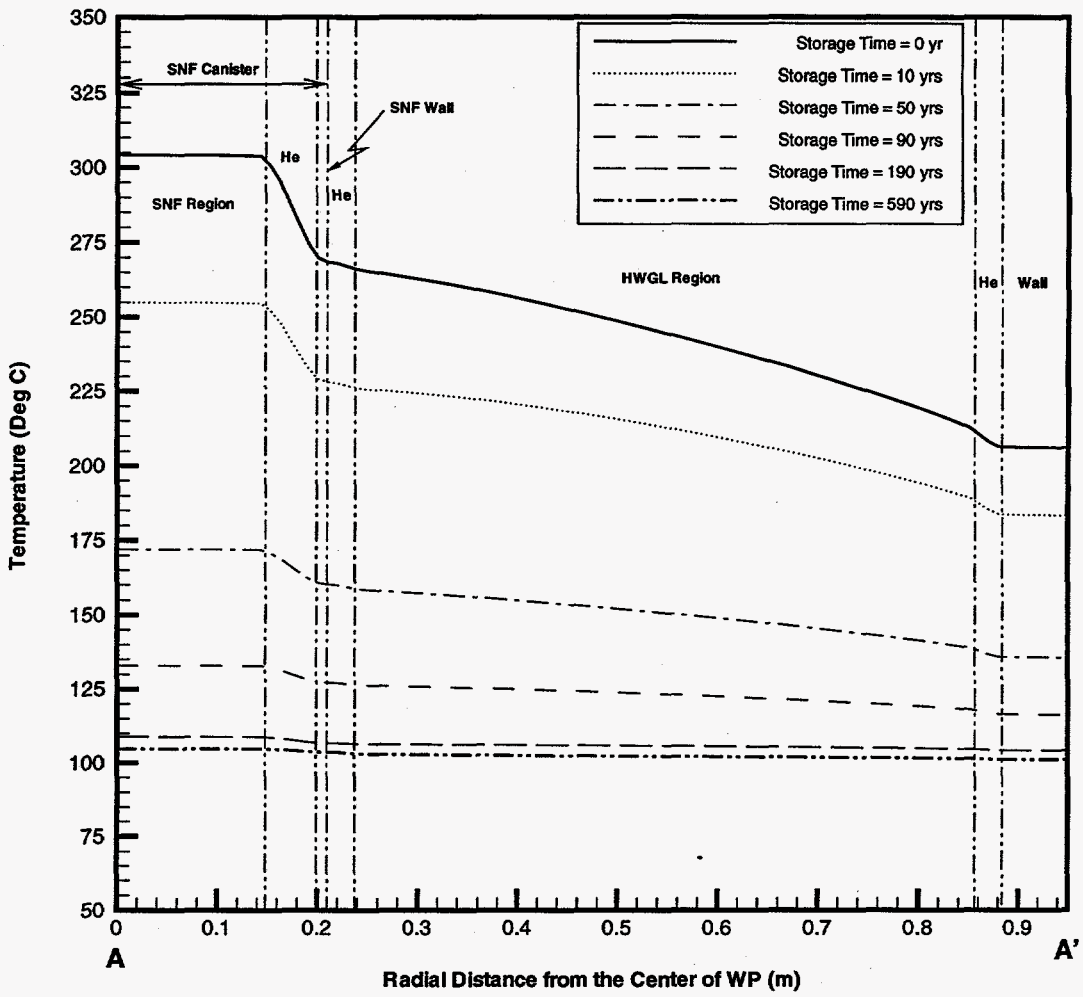


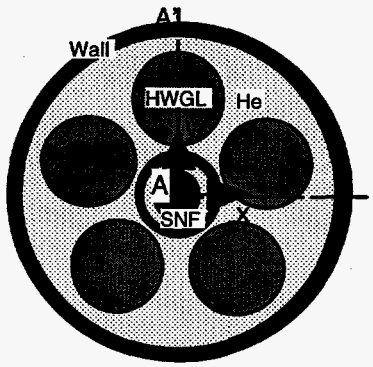


Figure 12. He-cooled codisposal WP temperature distribution for various storage times based on the baseline model.

## Conclusions

Two models were developed to assess the thermal performance of the interim dry storage and geological codisposal WP designs using computational heat transfer approach. The model predictions of temperature and flow velocity distributions were made for four He-cooled canisters with $h_{wall}$ = 6.4 to 19.6 W/m$^2$K and q''' = 25 to 35 kW/m$^3$ (Case-1 to Case -4) and three $N_2$-cooled canisters with $h_{wall}$ = 6.1 to 13.4 W/m$^2$K and q''' = 22 to 25 kW/m$^3$ (Case-5 to Case-7). It is noted that temperature and velocity gradients near the conduction-convection interface within a thermal boundary layer for $N_2$-cooled design is much larger than those of He-cooled design. The results show that the use of nitrogen as a backfill gas is not a huge disadvantage although its thermal conductivity is much lower than that of helium. A natural convective cooling mechanism for both cases was found to be very important in assessing the thermal performance of the four Al-SNF assemblies contained in the dry storage canister. The computational results are consistent with natural convection phenomena in the literature (Kays and Crawford, 1980) as shown in Fig. 10. All the benchmarking results are also shown to be in good agreement with the SRS test data.

The present analysis used well-defined decay heat loads for the SNF canister and HWGL regions. Reference model boundary conditions were provided by the WP performance requirements of a drift tunnel repository. In this project, a dry spent nuclear fuel disposal option was considered for the alternative SNF treatment program using the codisposal WP configuration. The thermal performance analyses for various design options of the present codisposal WP configuration were performed mainly using the baseline model because of the computational efficiency. The results of the baseline model showed that the direct disposal configuration with a helium-filled WP satisfied the present waste acceptance criteria (WAC) for the WP design in terms of the peak temperature criterion, $T_{max} \leq 350$ °C, under the reference boundary conditions.

## Acknowledgment

This research was performed by Westinghouse Savannah River Company under contract for the Department of Energy.

## References

1. CFX 4.1 User Guide, AEA Technology, 1995.
2. A. J. Chapman, *Heat Transfer*, Third Edition, Macmillan Publishing Co., Inc,, (1974).
3. Kays, W. M. and Crawford, M. E., *Convective Heat and Mass Transfer*, Second Edition, McGraw-Hill Book Company, 1980.
4. Lee, S. Y., "CFD Modeling of Natural Convection within Dry Spent Nuclear Fuel Storage Canister", ANS Proceedings of 1996 National Heat Transfer Conference, August 3-6, 1996, HTC-Vol.9, pp.213-224.
5. McAdams, W. H., *Heat Transmission*, Third Edition, McGraw-Hill Book Company, 1954.